Journal of Chemical&Engineering Data

pubs.acs.org/jced Article

Intensification of High Boiling Point Organic Solvents on SO_2 Absorption in Deep Eutectic Solvents Formed by Hydroxypyridine and 1-Butyl-3-methylimidazolium Chloride

Bin Jiang, Congcong Zhang, Xiaowei Tantai,* Na Yang,* Luhong Zhang, Yongli Sun, and Xiaoming Xiao

Cite This: *J. Chem. Eng. Data* 2022, 67, 3435−3442 Read Online

ACCESS | Metrics & More | Article Recommendations | Supporting Information

ABSTRACT: A series of hydrogen bond donors (HBDs) functionalized deep eutectic solvents (DESs) containing both physical and chemical action sites were synthesized by hydroxypyridine with different structures and proportions plus 1-butyl-3-methylimidazolium chloride (BmimCl). The effects of temperature, partial pressure, HBDs structure, and water content on SO_2 absorption were investigated, and 4-hydroxypyridine (4-Op)/BmimCl (1:2) exhibited the highest SO_2 absorption capacity. In order to decrease the viscosity of absorbent and increase the applicability of 4-Op/BmimCl (1:2), the SO_2 absorption capacities in four hybrid absorbents based on 4-Op/BmimCl (1:2) and four high boiling point organic solvents [sulfone, dimethyl sulfoxide (DMSO), *N*-methylpyrrolidone (NMP), and 1-methylimidazole (NMI)] were further studied and compared. 4-Op/BmimCl (1:2)-(NMI) showed the best absorption performance; the addition of NMI significantly decreased the viscosity of the absorbent, and the absorption capacity of absorbent was also improved compared with that of pure 4-Op/BmimCl (1:2) absorbent. The SO_2 absorption capacity of hybrid absorbents (mass fraction of NMI ω = 0.3) could reach 1.23 g SO_2/g absorbent at 100 kPa SO_2 and 293.15 K, and the viscosity of the absorbent before absorption was only 12 mPa·s at 298.15 K. The gravimetric absorption capacity and desorption performance of hybrid absorbents did not change in the continuous absorption−desorption cycle experiments. Furthermore, the results of quantum chemical calculation and spectral analysis showed that there were physicochemical mixing interactions between pure DESs and SO_2.

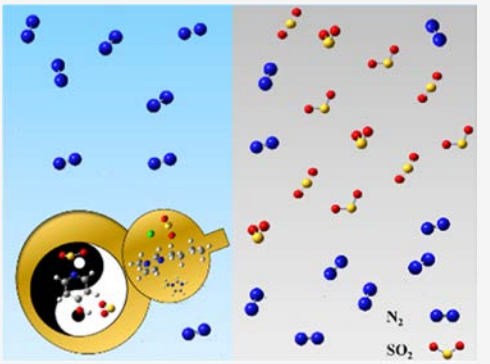

1. INTRODUCTION

Acid rain haze and photochemical smog caused by SO_2 released from fossil fuel burning cause serious harm to ecological environment and human health. With the increasingly strict sulfur dioxide emission standards, the removal of sulfur dioxide from industrial waste gas has attracted increasing attention. The inherent shortcomings of traditional technologies (lime-limestone method and ammonia washing technology) are driving researchers to develop new materials and processes that can effectively and reversibly remove SO_2 to protect the environment.[1,2]

Deep eutectic solvents (DESs) have attracted broad attention over the past decades as a kind of ionic liquid analogues. DESs are usually prepared from two or more components, namely, hydrogen bond acceptors (HBAs) and hydrogen bond donors (HBDs). Quaternary phosphonium salts or quaternary ammonium salts are commonly used as HBAs, while alcohols, carboxylic acids, and amides are used as HBDs. The formation of intermolecular hydrogen bonds between the individual component results in a significant decrease in the melting point of DESs.[3] DESs have played a significant role in acid gas absorption, such as CO_2,[4] NO,[5] and SO_2.[6,7] Jiang et al. investigated the SO_2 absorption capacity in different phosphonium-based HBAs; methyl-triphenyl phosphonium bromide (MTPB) with shorter carbon chain length substituents exhibited the best SO_2 absorption capacity (0.2 g SO_2/g DESs at 0.05 vol % SO_2 and 303.15 K).[8] Jiang et al. investigated the effects of several different HBAs (EmimCl, BmimCl, BmimBr, $N_{4444}Cl$, and $P_{4444}Cl$) on SO_2 absorption capacity.[6] Among them, EmimCl and BmimCl exhibited competitive SO_2 absorption capacity. Compared with EmimCl, BmimCl had similar SO_2 capacity and relatively lower cost; BmimCl was selected as HBA for the subsequent investigations. Generally, SO_2 chemisorptions by these functionalized DESs are based on the single-site interaction between the electronegative nitrogen and SO_2.[9,10] The molecule containing hydroxyl group can physically absorb SO_2 through the formation of an −OH···O═S═O hydrogen bond.[11] Therefore, we can regulate the number and type of interaction

Received: May 25, 2022
Accepted: September 21, 2022
Published: October 5, 2022

https://doi.org/10.1021/acs.jced.2c00334
J. Chem. Eng. Data 2022, 67, 3435−3442

sites to adjust the adsorption and desorption capacity of SO_2.[12,13] In addition, most DESs or ionic liquids have high viscosity and are difficult to transport in pipelines in practical applications. Therefore, combining DESs with organic solvents or water to construct mixed absorbent may be an attractive approach.[14,15]

Based on the above analysis, we prepared a series of hydroxypyridine DESs. The effects of temperature, SO_2 partial pressure, DES composition, and the type and proportion of organic solvents on the SO_2 absorption performance were investigated. Thermogravimetric analysis (TGA) and five continuous absorption−desorption cycles showed that the stability and reversibility of absorbents were high. The SO_2/CO_2 selectivity and physical properties of DESs were also discussed. Furthermore, the physicochemical mixing interactions between hydroxypyridine-based DESs and SO_2 were verified by quantum chemical calculation and spectral analysis.

2. EXPERIMENTAL SECTION

2.1. Materials and Characterization. The chemical structures and abbreviations of chemicals used are shown in Figure 1. 2-Hydroxypyridine (99%, CAS no. 142-08-5), 3-hydroxypyridine (99%, CAS no. 109-00-2), 4-hydroxypyridine (99%, CAS no. 626-64-2), 1-methylimidazole (98%, CAS no. 616-47-7), sulfolane (99%, CAS no. 126-33-0), *N*-methylpyrrolidone (NMP) (99%, CAS no. 872-50-4), dimethyl sulfoxide (99%, CAS no. 67-68-5), and 1-butyl-3-methylimidazolium chloride (98+%, CAS no. 79917-90-1) were obtained from he owns OPDE Technologies, LLC. All chemicals used were vacuum-dried for 12 h to remove trace moisture before DESs preparation. SO_2 (99.95%), CO_2 (99.95%), and N_2 (99.99%) were purchased from Tianjin Dongxiang Specialty Gases Co., Ltd. Standard gas mixture of 2000 ppm SO_2 and N_2 was purchased from Tianjin Boliming Technology Co., Ltd, and other SO_2 mixtures with partial pressure were obtained by using N_2 as the equilibrium gas.

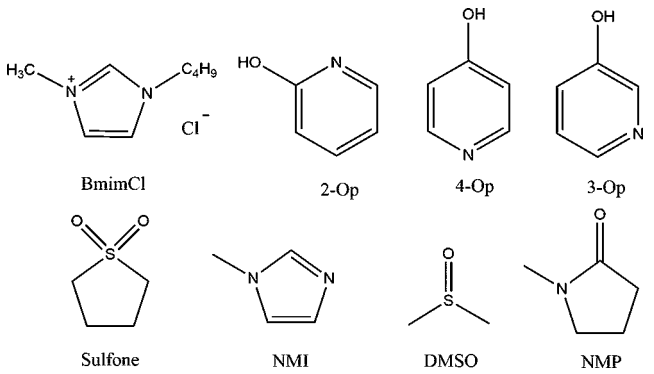

Figure 1. Chemical structures and abbreviations for synthesizing hybrid absorbents.

The viscosities of hydroxypyridine-based DESs and hybrid absorbents were characterized using a rotary viscometer (Brookfield DV-II + Pro, America) at 293.15 K and calibrated with standard silicone oil before measurement. All samples were repeated three times to calculate the average viscosities. The thermostability of hydroxypyridine-based DESs was analyzed by TGA (NETZSCH, TG209F3) from room temperature to 673.15 K at a heating rate of 10 K/min under nitrogen atmosphere, and the decomposition temperatures were characterized by using the TGA curves. A 500 MHz Bruke spectrometer (AVANCE III, Germany) was used to characterize the ^{1}H NMR spectra in DMSO-d_6, and TMS was selected as an internal standard. A Bruker TENSOR II Fourier transform spectrometer was used to obtain FT-IR spectra in the wavenumber range of 400−4000 cm^{-1}.

2.2. Preparation of the Deep Eutectic Solvents. The preparation method of DESs in this article was consistent with that reported in previous literature.[6] All DESs used in this article were prepared by mixing HBDs (2-Op, 3-Op, and 4-Op) with HBAs (BmimCl) in a certain molar ratio and then stirred at 343.15 K until all the solid particles formed a transparent liquid. Subsequently, the prepared DESs were vacuum-dried at 353.15 K for 24 h to remove the possible volatile organic compounds and traces moisture. The AKF-2010 Karl Fischer moisture titrator (Hogon Co., Ltd.) was used to measure the water content (Table S1).

2.3. SO_2 Absorption and Absorbent Regeneration. The method and equipment of SO_2 absorption and desorption operations were consistent with those of previous literature.[6] Mass flowmeters were used to regulate the flow of gas in high-pressure cylinders to obtain simulated flue gas with different SO_2 partial pressures. The simulated flue gas with a flow rate of 100 mL/min at 100 kPa was bubbled into absorbent (about

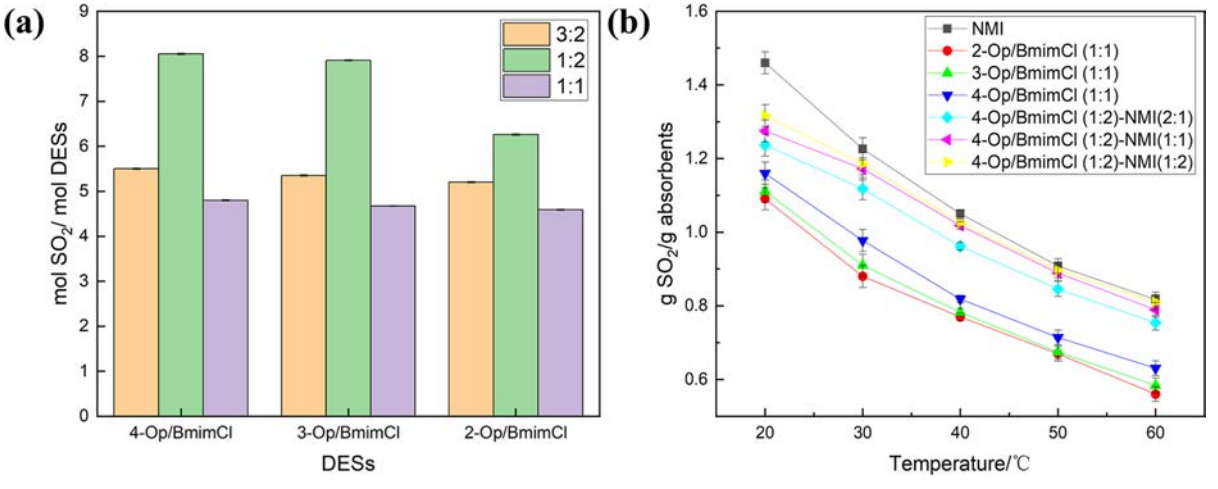

Figure 2. Effect of (a) HBDs/HBAs mole ratio; (b) temperature and types of HBDs on SO_2 absorption at 100 kPa.

https://doi.org/10.1021/acs.jced.2c00334
J. Chem. Eng. Data 2022, 67, 3435−3442

1.0 g) in a glass container, which was immersed in a constant-temperature water or oil bath. Electronic balance (Mettler Toledo AL204, with an accuracy of 0.1 mg) was used to determine the solubility of SO_2 at regular intervals during the absorption process. Desorption operations were conducted at 353.15 K in nitrogen atmosphere, and each measurement was repeated three times. The repeatability was better than ±2%, and it was estimated that the uncertainty of the results was less than ±2.5%.

3. RESULTS AND DISCUSSION

3.1. Physical Properties. Viscosity plays an important role in the process of mass and heat transfer, and lower viscosity of absorbents is more conducive to industrial applications. The measured viscosities of DESs before and after SO_2 absorption are summarized in Table S2. The viscosities of hybrid absorbents with different mass fractions of NMI are shown in Figure S1; the addition of NMI could effectively reduce the viscosity of DESs. The viscosities of pure DESs decreased obviously after 100 kPa SO_2 absorption, which was related to the destruction of the hydrogen bond between HBDs and HBAs by SO_2.[16] The viscosity of 4-Op/BmimCl (1:2) or 3-Op/BmimCl (1:2) increased after capturing low concentration SO_2 (0.2 vol %), which indicated that there was a chemical interaction between DESs and SO_2, which will be further explored by spectral analysis.[9] Also, the hybrid absorbents exhibited lower viscosity both before and after 100 kPa SO_2 absorption. In addition, the melting point of the mixture was lower than that of the components, conforming to the definition of DESs (as stated by the supplier: BmimCl, 343.15 K; 4-Op, 423.15 K; 3-Op, 403.15 K; 2-Op, 380.15 K), and all the prepared hydroxypyridinyl-based DESs were room temperature DESs.

3.2. SO_2 Absorption. As shown in Figure 2a, the influence of HBD/HBA mole ratio in the range of 3:2−1:2 on SO_2 absorption was investigated at 100 kPa SO_2 and 293.15 K (stable DESs could not be formed under experimental conditions when the HBA/HBD mole ratio was 1:2). Notably, molar absorption capacities of 4-Op/BmimCl (1:2) could reach 8.05 mol SO_2/mol DES. Obviously, as the 4-Op/BmimCl molar ratio decreased from 3:2 to 1:2, the saturated SO_2 molar absorption capacities of 4-Op/BmimCl DESs decreased and then increased, corresponding to 5.50, 4.80, and 8.05 mol SO_2/mol DES, respectively. The results demonstrated that both HBAs and HBDs played an important role in SO_2 absorption.

The effects of temperatures and types of HBDs on the absorption capacities of SO_2 by pure DESs and hybrid absorbents were explored at 100 kPa SO_2, and the results are showed in Figure 2b. It was found that the saturated absorption capacities of SO_2 by all absorbents significantly decreased with the rise of temperature. Precisely, as the temperature increased from 293.15 to 333.15 K, the saturated SO_2 absorption capacities of 4-Op/BmimCl (1:1), 3-Op/BmimCl (1:1), and 2-Op/BmimCl (1:1) decreased from 1.14 to 0.63, 1.11 to 0.58, and 1.09 to 0.56 g SO_2/g DES, respectively. The order of SO_2 absorption capacity was 4-Op/BmimCl > 3-Op/BmimCl > 2-Op/BmimCl. The results demonstrated that the site of N atoms may affect the absorption capacity of SO_2, and the SO_2 captured by pure DESs and hybrid absorbents could be facilely stripped out by heating. Based on the above analysis, 4-Op/BmimCl (1:2) exhibited better absorption performance, which will be further studied.

As shown in Table S3 and Figure S5, the SO_2 absorption capacities of hybrid absorbents that 4-Op/BmimCl (1:2) mixed with NMP, DMSO, NMI and Sulfone respectively at the mass ratio of 1:2 were investigated. The SO_2 gravimetric absorption capacities of hybrid absorbents were 1.04, 1.21, 1.31, and 0.71 g SO_2/g absorbents, respectively. Only the hybrid absorbent corresponding to NMI did not generate solid substances, while the other hybrid absorbents generated precipitation at the bottom. Therefore, as shown in Figure 2b, the SO_2 absorption capacities of NMI hybrid absorbents with different mass ratios were further explored. When the mass ratio of DES-NMI was 1:2, it exhibited competitive SO_2 gravimetric absorption capacity (1.31 g SO_2/g absorbent at 100 kPa SO_2 and 293.15 K). Figure S6 indicates that the addition of NMI reduced the thermal stability of DESs. With the rise of temperature, the volatilization of organic solvents causes the loss of desorption energy consumption and environmental pollution, so the proportion of organic solvents should not be too high.

Table S6 shows SO_2 absorption capacity of 4-Op/BmimCl (1:2) and 3-Op/BmimCl (1:2) at different SO_2 partial pressures. As depicted in Figure 3, the SO_2 partial pressure

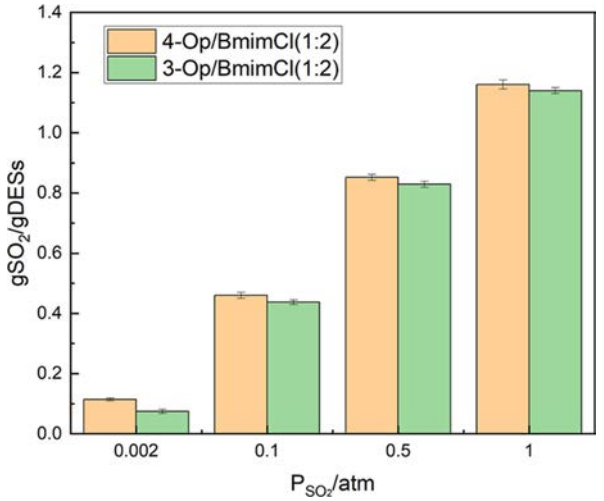

Figure 3. Effect of SO_2 partial pressure on SO_2 absorption performance at 293.15 K.

took an active effect on SO_2 absorption capacities. In particular, gravimetric absorption capacities of 4-Op/BmimCl (1:2) and 3-Op/BmimCl (1:2) increased from 0.11 to 1.16 g SO_2/g DES and 0.07 to 1.14 g SO_2/g DES as the partial pressure of SO_2 increased from 0.2 to 100 kPa at 293.15 K, respectively. The results indicated that the SO_2 absorbed by DESs could be desorbed by bubbling N_2.

As depicted in Figure 4, the influence of HBD/HBA mole ratio on SO_2 absorption was investigated at 293.15 K and 0.2 kPa [in the process of absorption, 3-Op/BmimCl (3:2) and 4-Op/BmimCl (3:2) became turbidity gradually, and solid particles were generated, so absorption could not be completed]. Interestingly, as the molar ratio of 4-Op/BmimCl declined, the equilibrium gravimetric absorption capacities of SO_2 in 4-Op/BmimCl DESs (1:1 and 1:2) decreased, corresponding to 0.15 and 0.11 g SO_2/g DES, respectively.

https://doi.org/10.1021/acs.jced.2c00334
J. Chem. Eng. Data 2022, 67, 3435−3442

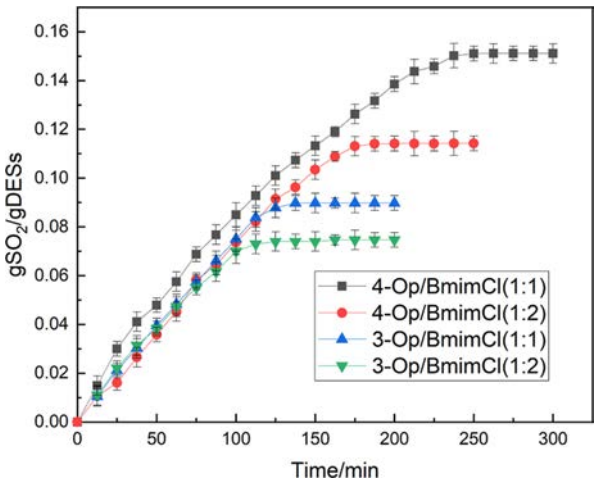

Figure 4. Effect of the HBD/HBA molar ratio on SO_2 absorption performance at 0.2 kPa SO_2.

The results showed that HBDs played a vital role in SO_2 absorption under low partial pressure.

3.3. Comparison with Other DESs That Chemically Absorb SO_2. The SO_2 absorption capacities in representative DESs and ILs reported previously are listed in Table 1. The SO_2 mass absorption capacities of DESs prepared in this work are higher than most DESs and ILs reported in the literature. Remarkably, the SO_2 gravimetric absorption capacities of 4-Op/BmimCl (1:2) could reach up to 1.16 and 0.46 g SO_2/g DES at 293.15 K under 100 and 10 kPa, respectively. Moreover, all the SO_2 absorbed in hydroxypyridine-based DESs could be desorbed easily, exhibiting remarkable desorption effect than other absorbents that chemically absorb SO_2. It is pointed out that some studies have shown that BmimCl has potential toxicity and can cause DNA damage to organisms.[17] In order to reduce the proportion of BmimCl and increase the application performance of the DESs, we developed four hybrid absorbents, among which the SO_2 absorption capacity of hybrid absorbents (mass fraction of NMI ω = 0.3) could reach 1.23 g SO_2/g absorbent at 100 kPa SO_2 and 293.15 K. Therefore, compared with the previously reported DESs and ILs, the studied DESs and hybrid absorbents showed better absorption and desorption performance, which had great application potential. Therefore, the proportion of IL in the absorbent should be reduced in practical application, and the development of more green and environmentally friendly absorbent is also the direction of our future efforts.

In addition, the SO_2/CO_2 selectivity of 4-Op/BmimCl (1:1) and 3-Op/BmimCl (1:1) was also investigated. Table S4 shows the CO_2 absorption capacity of 4-Op/BmimCl (1:1) and 3-Op/BmimCl (1:1) at 313.15 K with a 100 kPa CO_2 flow rate of 50 mL/min. Concretely, the CO_2 molar absorption capacities of 4-Op/BmimCl (1:1) and 3-Op/BmimCl (1:1) were 0.26 and 0.21 mol CO_2/mol DESs, respectively. Thus, the SO_2/CO_2 selectivity was determined to be 11.9 and 14.5 (ratio of molar absorption of SO_2/CO_2).

3.4. Thermostability of DESs and Regeneration of Absorbents. The thermostability and regeneration of absorbents are significant for evaluating the potential of industrial application. The thermostabilities of 4-Op/BmimCl (1:2) and 3-Op/BmimCl (1:2) were examined by TGA. As shown in Figure S2, the thermal degradation temperatures (T_d, 5 wt % weight loss) of 4-Op/BmimCl (1:2) and 3-Op/BmimCl (1:2) were 509.15 and 481.15 K, respectively. The T_d values of hydroxypyridine-based DESs were higher than the regeneration temperatures, which indicated that hydroxypyridine-based DESs were sufficiently stable in the process of regeneration. Further, to evaluate the reusability of DESs and hybrid absorbents, five consecutive absorption and desorption cycles were performed at 293.15 K, 100 kPa, SO_2 at 50 mL/min and 353.15 K, 100 kPa, and N_2 at 50 mL/min, respectively. As depicted in Figure 5, the saturated weight absorption capacities and desorption remnants of DESs and

Table 1. Comparison of SO_2 Absorption Capacities of Different DESs and ILs[a]

absorbent (molar ratio)	temperature (K)	SO_2 capacity (g SO_2/g DES)			reference
		100 kPa	10 kPa	0.2 kPa	
DES[d]-NMI(2:1)[f]	293.15	1.23			this work
4-Op/BmimCl (1:2)	293.15	1.16	0.46	0.11	this work
3-Op/BmimCl (1:2)	293.15	1.14	0.43	0.07	this work
4-Op/BmimCl (1:1)	293.15	1.11		0.15	this work
Gly/PPZBr (4:1)	293.15	0.42	0.15	0.10[b]	18
TBAB + CPL (1:2)	298.15	0.22			19
[Et2NEMim][Tetz]	293.15	1.10	0.47		20
EmimCl + EG (1:1)	293.15	1.03		0.047	21
EmimCl + SN (1:1)	293.15	1.13		0.12	22
EmimCl + TEG (6:1)	293.15	1.25	0.54		23
BmimCl-EU (2:1)	293.15	1.18			6
EG-MTPB (4:1)	303.15			0.2[e]	8
BmimCl−AA (1:1)	293.15	1.00	0.30		24
[P_{66614}][NPA]	298.25	0.37	0.13	0.04[b]	13
Bet/EG (1:3)	313.15	0.366	0.070[b]		25
ChCl/thiourea (1:1)	303.15	0.70	0.09[c]		26
ChCl/Gly (1:1)	293.15	0.678	0.153		27
CPL/KSCN (3:1)	293.15	0.61			28

[a]Standard uncertainties are $u(T)$ = 0.1 K, $u(P_{total})$ = 0.2 kPa, $u(P_{partial})$ = 0.01 kPa, u(molar ratio) = 0.01, and $u(mass_{SO_2})$ = 0.01 g/g. [b]At 1 kPa. [c]At 20 kPa. [d]DES: 4-Op/BmimCl (1:2). [e]At 0.05 kPa. [f]Mass ratio.

https://doi.org/10.1021/acs.jced.2c00334
J. Chem. Eng. Data 2022, 67, 3435−3442

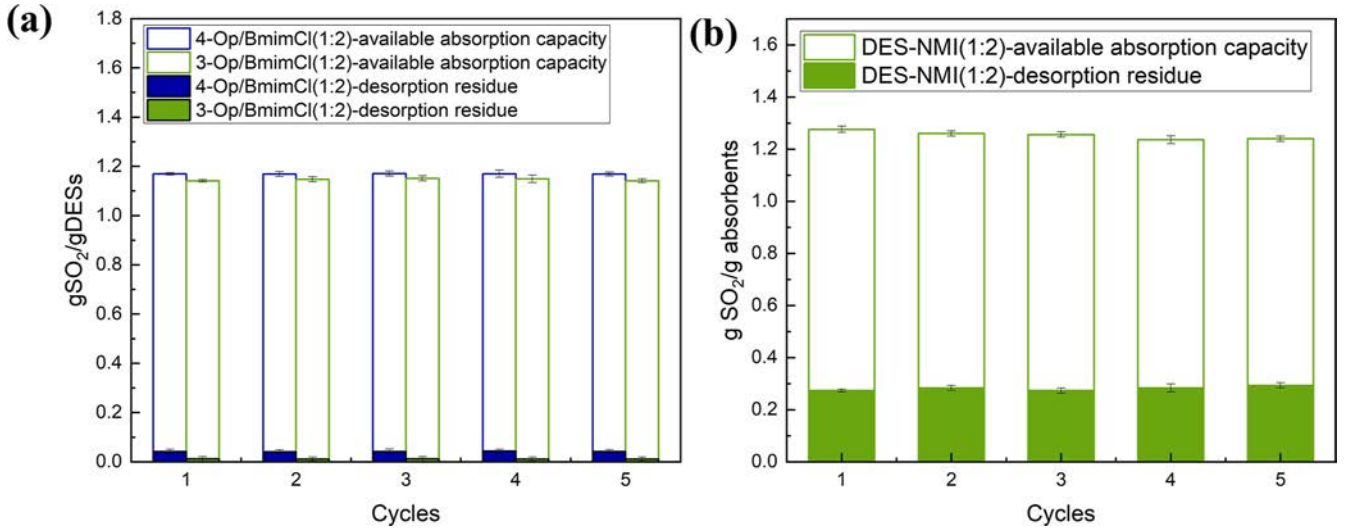

Figure 5. Five cycles of SO_2 absorption−desorption experiments by (a) pure DESs and (b) 4-Op/BmimCl (1:2) mixed with NMI in mass ratio.

hybrid absorbents did not alter obviously during five continuous absorption and desorption cycles. The results indicated that the SO_2 absorption by DESs and hybrid absorbents was reversible and could be used as a recyclable absorbent. Under the same conditions, the desorption efficiency of 4-Op/BmimCl (1:2), 3-Op/BmimCl (1:2), and DES-NMI (1:2) could reach 96.7, 99, and 78.5%, and the available SO_2 absorption capacities were about 1.12, 1.13, and 0.98 g SO_2/g absorbents, respectively. Although the available absorption capacity and desorption efficiency of hybrid absorbents were slightly lower than that of pure DES, the lower viscosity makes it more practical. The difference of absorption and desorption capacity between 4-Op/BmimCl (1:2) and 3-Op/BmimCl (1:2) will be further studied by quantum chemical calculation.

3.5. Spectroscopic Analysis. To explore the interactions of 4-Op/BmimCl (1:2) with SO_2, FT-IR spectra and ^{1}H NMR spectra of unreacted hydroxypyridine-based DESs as well as DESs saturated with SO_2 were characterized. As shown in Figure 6, compared with the FT-IR spectra of the virgin DESs, new peaks presented at 953 and 1722 cm^{-1} could be ascribed to S−O stretch vibrations and the interaction of N of the 4-Op with SO_2.[9,18,25] The above result indicated that there was chemical interactions between 4-Op/BmimCl (1:2) and SO_2. The typical characteristic peaks appeared at 536, 1128, and 1310 cm^{-1} after DESs saturated with SO_2, which could be ascribed to the bending vibration of SO_2[10,29,30] and the symmetrical and asymmetrical stretching vibration of S=O,[21,26] respectively. Generally, the symmetrical and asymmetrical stretching vibration of SO_2 were observed at 1145 and 1344 cm^{-1} in CCl_4, respectively.[31] The shifts indicated strong charge−transfer interaction between S atom of SO_2 and Cl^-.

As shown in Figure 7, compared with the virgin 4-Op/BmimCl (1:2), the typical chemical shifts of the protons of N−

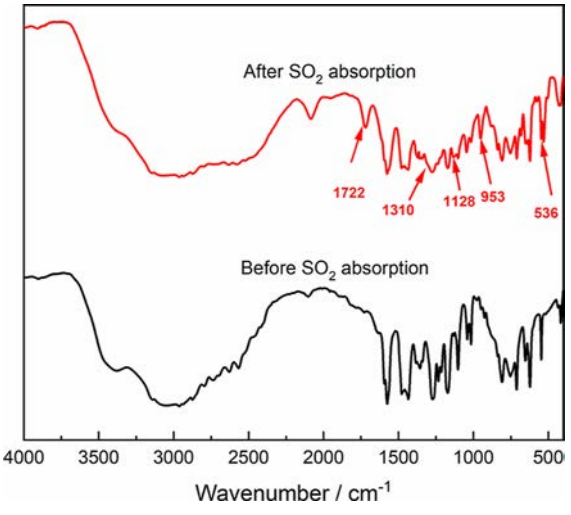

Figure 6. FT-IR spectra of 4-Op/BmimCl (1:2) before and after absorption of SO_2.

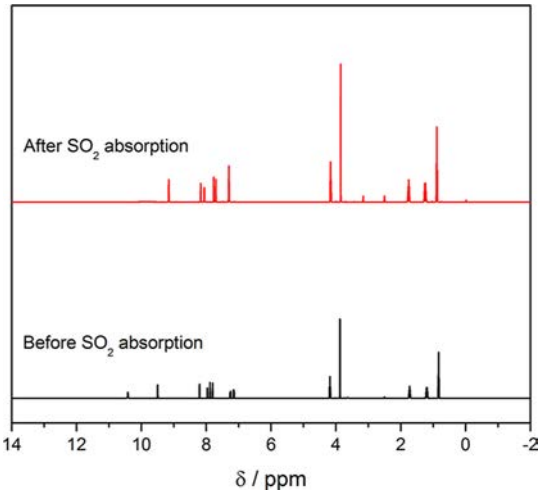

Figure 7. ^{1}H NMR spectra of 4-Op/BmimCl (1:2) before and after absorption of SO_2.

C_6−H (4-Op) moved downfield after hydroxypyridine-based DESs saturated with SO_2. For instance, the chemical shifts of the protons at 7.97 ppm moved downfield to 8.06 ppm after DESs saturated with SO_2 (100 kPa), indicating that the N···SO_2 chemical interaction exists between 4-Op and SO_2.[18,32] It should be noticed that the chemical shifts of C_2−H (BmimCl) at 9.5 ppm moved upfield to 9.16 ppm; besides, the intensities of chemical shifts of N−CH_3 and C_3H_7−CH_2 (BmimCl) at

https://doi.org/10.1021/acs.jced.2c00334
J. Chem. Eng. Data 2022, 67, 3435−3442

3.88 and 4.18 ppm increased, and the chemical signals became spike peaks, indicating that the hydrogen bond between the HBD and the HBA was broken. During the process of absorption, the viscosity of the absorbent decreased, which also confirmed that the hydrogen bond was broken. On the basis of FT-IR and ^{1}H NMR results, the 4-Op/BmimCl (1:2) interacted with SO_2 through mixed physicochemical interactions.

3.6. Quantum Chemical Calculations. Density functional theory calculations, at M06-2X/6-311+G(d,p),[33,34] with Gaussian 09[35] were used to demonstrate how the position between N and −OH affected the absorption−desorption properties of DESs, and the analysis of wave function was carried out with Multiwfn 3.8.[36] Details of quantum chemical calculations methods could be found in Supporting Information. The geometry optimization and NPA charge distribution of 2-Op, 3-Op, and 4-Op monomers were calculated, respectively, as shown in Supporting Information, Table S7. It could be seen from Figure S3 that the NPA atomic charge of N atoms in 3-Op was obviously lower than that of 4-Op. According to the mechanism of limited active sites,[37] it indicated that there were more potential absorption sites corresponding to N atoms in 4-Op, which was consistent with the experimental results that 4-Op had better absorption capacity than 3-Op. It was worth noting that the NPA atomic charge density of N atoms in 2-Op was also very high, but its relatively poor absorption performance may be due to the steric hindrance of hydroxyl group, which reduced the SO_2 absorption capacities.

The geometry optimization and interaction energies of optimized structures were calculated for 3-Op/BmimCl (1:1)-nSO_2 and 4-Op/BmimCl (1:1)-nSO_2 (n = 0,1,2) clusters, as shown in Figure 8. The interaction types and intensities in

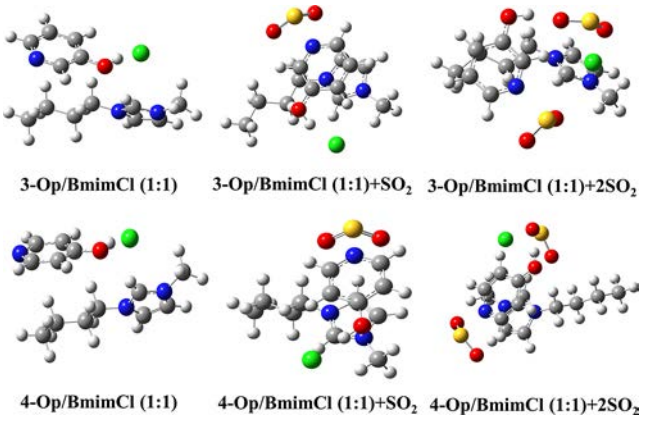

Figure 8. Optimized structures of DESs-nSO_2 (n = 0,1,2) complexes.

DESs-nSO_2 were quantitatively described, and topology analysis was carried out by using Multiwfn 3.8. As shown in Figure S3, there were many forms of hydrogen bonds between HBDs and BmimCl, such as H−O···H−HCC_2H_5, C_4−H···Cl^-, and so forth. It could be noted that when DESs bind a molecule of SO_2, the hydrogen bond between HBA and HBD is broken; for example, C_2−H···H−HCCH_3 converted to CH_3CH−H···O($^1SO_2$) and HC_4···H−HCC_3H_7 converted to (C_3H_7)CH−H···O^1($^1SO_2$). The above results were consistent with the spectral analysis results, indicating that there was a synergistic process of SO_2 absorption between HBDs and HBAs. Compared with the optimized 3-Op/BmimCl (1:1)-SO_2, 4-Op/BmimCl (1:1)-SO_2 had shorter intermolecular distance; the length of N···S was calculated as 2.19 and 2.14 Å, respectively, indicating that there was a stronger interaction between 4-Op/BmimCl (1:1) and SO_2. The interaction energies of 3-Op/BmimCl (1:1)-SO_2 and 4-Op/BmimCl (1:1)-SO_2 were calculated as −89.80 and −105.06 kJ/mol, respectively. The above results indicated that 3-Op/BmimCl (1:1) had weaker interaction with SO_2, which was consistent with the experimental results that 3-Op/BmimCl (1:1) had a better desorption performance.

In order to understand which regions of molecules were related to weak interactions more intuitively, the reduced density gradient (RDG) was used to visualize the weak interaction of DESs. The RDG isosurface coloring of interactions in geometry-optimized DES-nSO_2 clusters is shown in Figure 9. The blue areas represent halogen and

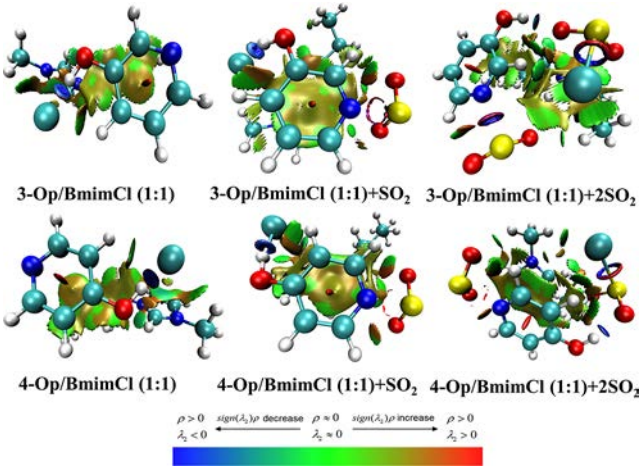

Figure 9. RDG isosurface coloring of interactions in DESs-nSO_2 clusters.

hydrogen bonding, the green areas represent the weaker van der Waals forces, and the red areas show the mutual exclusion effect between interacting atoms, which are mainly the strong steric hindrance of cage and ring structures.

As can be seen from the Figure 9, the weak interaction in the system was destroyed after SO_2 absorption, and the complete region becomes fragmented, which was in accordance with the experimental results that the viscosity of absorbents decreased during the experimental process. It should be noted that the mapping screened the points with electron densities greater than 0.05 a.u., and due to the strong interaction between N···S and Cl^-···S, the circular equivalence surface of the inner blue and the outer red appeared between them.

In order to further verify the results of geometry optimization, an analysis of electrostatic potential was carried out. It could be seen from Figure 10 that 3-Op/BmimCl (1:1) and 4-Op/BmimCl (1:1) showed semblable electrostatic potential distribution of molecules. Specifically, the electronegative areas were chiefly located near Cl^- and N atoms (HBDs) and O atoms, while the electronegative areas were chiefly located near H atoms, such as the C_2−H on the Im ring, C−H of HBDs, and branch chain of the Im ring. Consequently, it could be inferred that the electropositive S atoms in SO_2 tend to bind to Cl^- or N atoms (HBDs), while electronegative O atoms in SO_2 prefer to form hydrogen bond with H atoms. The results of electrostatic potential distribution

https://doi.org/10.1021/acs.jced.2c00334
J. Chem. Eng. Data 2022, 67, 3435−3442

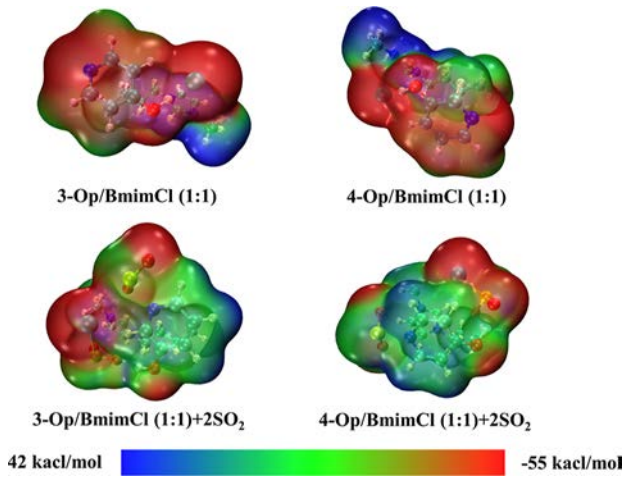

Figure 10. Electrostatic potential surface mapped on electron total density with an isovalue of 0.001.

were consistent with those of geometric optimization. The electrostatic maps of DES-2SO_2 verified the above deduction. The N atoms (HBDs) and chloride ions contacted with the sulfur region with positive electrostatic potential of SO_2, while the positive parts of other molecules contacted with the oxygen region with negative electrostatic potential of SO_2, so that SO_2 was firmly adsorbed through electrostatic interaction. Based on the above analysis, it was suggested that the excellent SO_2 desorption and absorption performance of hydroxypyridine-based DESs on account of the weaker interaction between SO_2 and DESs and the synergism between HBDs and HBAs promotes the capture of SO_2.

4. CONCLUSIONS

A series of HBD-functionalized DESs containing both physical and chemical action sites were synthesized, and the absorption of SO_2 was investigated under different temperatures, water contents, and partial pressures. It is worth noting that 4-Op/BmimCl (1:2) showed an extremely high SO_2 capacity up to 1.21 and 0.14 g SO_2/g DES at 293.15 K under 100 and 0.2 kPa, respectively. Furthermore, the effects of the type and proportion of organic solvents on the viscosity of 4-Op/BmimCl (1:2) and the absorption capacity of SO_2 were investigated. The SO_2 absorption capacity of hybrid absorbents (mass fraction of NMI ω = 0.3) could reach 1.23 g SO_2/g absorbent at 100 kPa SO_2 and 293.15 K, and the viscosity of the absorbent before absorption was only 12 mPa·s at 298.15 K. The absorption mechanism between hydroxypyridine-based DESs and SO_2 was investigated by combining spectroscopic investigations with quantum chemical calculations. It was found that the increased SO_2 absorption capacity was attributed to multiple-site interactions and the synergism between HBDs and HBAs. Combining NMI with DESs provided a potential solution for the application of DES-based absorbents, a strategy that was attractive for the development of SO_2 absorbents.

■ ASSOCIATED CONTENT

Supporting Information

The Supporting Information is available free of charge at https://pubs.acs.org/doi/10.1021/acs.jced.2c00334.

Physical properties and water content of the studied DESs, TGA curves of 4-Op/BmimCl (1:2) and 3-Op/BmimCl (1:2), SO_2/CO_2 selectivity of the studied DESs, SO_2 solubility in DESs, details of quantum chemical calculations methods, topological parameters of the key interactions in DESs, and NPA charge distribution of monomers (PDF)

■ AUTHOR INFORMATION

Corresponding Authors

Xiaowei Tantai − *School of Chemical Engineering and Technology, Tianjin University, Tianjin 300072, P. R. China;* orcid.org/0000-0003-2925-0444; Phone: +86 22 27400199; Email: tantaixw@tju.edu.cn

Na Yang − *School of Chemical Engineering and Technology, Tianjin University, Tianjin 300072, P. R. China;* orcid.org/0000-0003-4888-5971; Email: yangnayna@tju.edu.cn

Authors

Bin Jiang − *School of Chemical Engineering and Technology, Tianjin University, Tianjin 300072, P. R. China*

Congcong Zhang − *School of Chemical Engineering and Technology, Tianjin University, Tianjin 300072, P. R. China*

Luhong Zhang − *School of Chemical Engineering and Technology, Tianjin University, Tianjin 300072, P. R. China;* orcid.org/0000-0002-7073-4793

Yongli Sun − *School of Chemical Engineering and Technology, Tianjin University, Tianjin 300072, P. R. China*

Xiaoming Xiao − *School of Chemical Engineering and Technology, Tianjin University, Tianjin 300072, P. R. China*

Complete contact information is available at: https://pubs.acs.org/10.1021/acs.jced.2c00334

Notes

The authors declare no competing financial interest.

■ ACKNOWLEDGMENTS

We are grateful for the financial support from the National Key R&D Program of China (no. 2016YFC0400406).

■ REFERENCES

(1) Gutiérrez Ortiz, F. J.; Vidal, F.; Ollero, P.; Salvador, L.; Cortés, V.; Giménez, A. Pilot-Plant Technical Assessment of Wet Flue Gas Desulfurization Using Limestone. *Ind. Eng. Chem. Res.* **2006**, *45*, 1466−1477.

(2) Zheng, Y.; Kiil, S.; Johnsson, J. E. Experimental investigation of a pilot-scale jet bubbling reactor for wet flue gas desulphurisation. *Chem. Eng. Sci.* **2003**, *58*, 4695−4703.

(3) Zhang, Q.; De Oliveira Vigier, K.; Royer, S.; Jérôme, F. Deep eutectic solvents: syntheses, properties and applications. *Chem. Soc. Rev.* **2012**, *41*, 7108−7146.

(4) Trivedi, T. J.; Lee, J. H.; Lee, H. J.; Jeong, Y. K.; Choi, J. W. Deep eutectic solvents as attractive media for CO2 capture. *Green Chem.* **2016**, *18*, 2834−2842.

(5) Sun, Y.; Wei, G.; Tantai, X.; Huang, Z.; Yang, H.; Zhang, L. Highly Efficient Nitric Oxide Absorption by Environmentally Friendly Deep Eutectic Solvents Based on 1,3-Dimethylthiourea. *Energy Fuels* **2017**, *31*, 12439−12445.

(6) Jiang, B.; Zhang, H.; Zhang, L.; Zhang, N.; Huang, Z.; Chen, Y.; Sun, Y.; Tantai, X. Novel Deep Eutectic Solvents for Highly Efficient and Reversible Absorption of SO2 by Preorganization Strategy. *ACS Sustainable Chem. Eng.* **2019**, *7*, 8347−8357.

(7) Hou, S.; Zhang, C.; Jiang, B.; Zhang, H.; Zhang, L.; Yang, N.; Zhang, N.; Xiao, X.; Tantai, X. Investigation of Highly Efficient and

Reversible Absorption of SO2 Using Ternary Functional Deep Eutectic Solvents. *ACS Sustainable Chem. Eng.* **2020**, *8*, 16241−16251.
(8) Zhao, Y.; Dou, J.; Wei, A.; Khoshkrish, S.; Yu, J. Highly efficient and reversible low-concentration SO2 absorption in flue gas using novel phosphonium-based deep eutectic solvents with different substituents. *J. Mol. Liq.* **2021**, *340*, 117228.
(9) Zhang, K.; Ren, S.; Yang, X.; Hou, Y.; Wu, W.; Bao, Y. Efficient absorption of low-concentration SO 2 in simulated flue gas by functional deep eutectic solvents based on imidazole and its derivatives. *Chem. Eng. J.* **2017**, *327*, 128−134.
(10) Cui, G.; Yang, D.; Qi, H. Efficient SO2 Absorption by Anion-Functionalized Deep Eutectic Solvents. *Ind. Eng. Chem. Res.* **2021**, *60*, 4536−4541.
(11) Yang, S.; Sun, J.; Ramirez-Cuesta, A. J.; Callear, S. K.; David, W. I.; Anderson, D. P.; Newby, R.; Blake, A. J.; Parker, J. E.; Tang, C. C.; Schröder, M. Selectivity and direct visualization of carbon dioxide and sulfur dioxide in a decorated porous host. *Nat. Chem.* **2012**, *4*, 887−894.
(12) Cui, G.; Wang, C.; Zheng, J.; Guo, Y.; Luo, X.; Li, H. Highly efficient SO2 capture by dual functionalized ionic liquids through a combination of chemical and physical absorption. *Chem. Commun.* **2012**, *48*, 2633−2635.
(13) Cui, G.; Zhang, F.; Zhou, X.; Huang, Y.; Xuan, X.; Wang, J. Acylamido-Based Anion-Functionalized Ionic Liquids for Efficient SO2 Capture through Multiple-Site Interactions. *ACS Sustainable Chem. Eng.* **2015**, *3*, 2264−2270.
(14) Huang, K.; Lu, J.-F.; Wu, Y.-T.; Hu, X.-B.; Zhang, Z.-B. Absorption of SO2 in aqueous solutions of mixed hydroxylammonium dicarboxylate ionic liquids. *Chem. Eng. J.* **2013**, *215−216*, 36−44.
(15) Zhou, Z.; Jing, G.; Zhou, L. Characterization and absorption of carbon dioxide into aqueous solution of amino acid ionic liquid [N1111][Gly] and 2-amino-2-methyl-1-propanol. *Chem. Eng. J.* **2012**, *204−206*, 235−243.
(16) Ren, S.; Hou, Y.; Wu, W.; Liu, Q.; Xiao, Y.; Chen, X. Properties of Ionic Liquids Absorbing SO2 and the Mechanism of the Absorption. *J. Phys. Chem. B* **2010**, *114*, 2175−2179.
(17) Zhang, C.; Shao, Y.; Zhu, L.; Wang, J.; Wang, J.; Guo, Y. Acute toxicity, biochemical toxicity and genotoxicity caused by 1-butyl-3-methylimidazolium chloride and 1-butyl-3-methylimidazolium tetrafluoroborate in zebrafish (Danio rerio) livers. *Environ. Toxicol. Pharmacol.* **2017**, *51*, 131−137.
(18) Cui, G.; Liu, J.; Lyu, S.; Wang, H.; Li, Z.; Wang, J. Efficient and Reversible SO2 Absorption by Environmentally Friendly Task-Specific Deep Eutectic Solvents of PPZBr + Gly. *ACS Sustainable Chem. Eng.* **2019**, *7*, 14236−14246.
(19) Guo, B.; Duan, E.; Ren, A.; Wang, Y.; Liu, H. Solubility of SO2 in Caprolactam Tetrabutyl Ammonium Bromide Ionic Liquids. *J. Chem. Eng. Data* **2009**, *55*, 1398−1401.
(20) Yang, D.; Hou, M.; Ning, H.; Ma, J.; Kang, X.; Zhang, J.; Han, B. Reversible Capture of SO2through Functionalized Ionic Liquids. *ChemSusChem* **2013**, *6*, 1191−1195.
(21) Yang, D.; Han, Y.; Qi, H.; Wang, Y.; Dai, S. Efficient Absorption of SO2 by EmimCl-EG Deep Eutectic Solvents. *ACS Sustainable Chem. Eng.* **2017**, *5*, 6382−6386.
(22) Yang, D.; Zhang, S.; Jiang, D.-e. Efficient Absorption of SO2 by Deep Eutectic Solvents Formed by Biobased Aprotic Organic Compound Succinonitrile and 1-Ethyl-3-methylimidazolium Chloride. *ACS Sustainable Chem. Eng.* **2019**, *7*, 9086−9091.
(23) Yang, D.; Zhang, S.; Jiang, D. E.; Dai, S. SO2absorption in EmimCl-TEG deep eutectic solvents. *Phys. Chem. Chem. Phys.* **2018**, *20*, 15168−15173.
(24) Zhao, T.; Liang, J.; Zhang, Y.; Wu, Y.; Hu, X. Unexpectedly efficient SO2 capture and conversion to sulfur in novel imidazole-based deep eutectic solvents. *Chem. Commun.* **2018**, *54*, 8964−8967.
(25) Zhang, K.; Ren, S.; Hou, Y.; Wu, W. Efficient absorption of SO2 with low-partial pressures by environmentally benign functional deep eutectic solvents. *J. Hazard. Mater.* **2017**, *324*, 457−463.
(26) Sun, S.; Niu, Y.; Xu, Q.; Sun, Z.; Wei, X. Efficient SO2 Absorptions by Four Kinds of Deep Eutectic Solvents Based on Choline Chloride. *Ind. Eng. Chem. Res.* **2015**, *54*, 8019−8024.
(27) Yang, D.; Hou, M.; Ning, H.; Zhang, J.; Ma, J.; Yang, G.; Han, B. Efficient SO_2 absorption by renewable choline chloride−glycerol deep eutectic solvents. *Green Chem.* **2013**, *15*, 2261.
(28) Liu, B.; Wei, F.; Zhao, J.; Wang, Y. Characterization of amide−thiocyanates eutectic ionic liquids and their application in SO_2 absorption. *RSC Adv.* **2013**, *3*, 2470.
(29) Chen, Y.; Jiang, B.; Dou, H.; Zhang, L.; Tantai, X.; Sun, Y.; Zhang, H. Highly Efficient and Reversible Capture of Low Partial Pressure SO2 by Functional Deep Eutectic Solvents. *Energy Fuels* **2018**, *32*, 10737−10744.
(30) Wang, C.; Bi, Q.; Huo, Y.; Zhang, Z.; Tao, D.; Shen, Y.; Zhu, Q.; Chen, Z.; Li, H.; Zhu, W. Investigation of Amine-Based Ternary Deep Eutectic Solvents for Efficient, Rapid, and Reversible SO2 Absorption. *Energy Fuels* **2021**, *35*, 20406−20410.
(31) van Dam, M. H. H.; Lamine, A. S.; Roizard, D.; Lochon, P.; Roizard, C. Selective Sulfur Dioxide Removal Using Organic Solvents. *Ind. Eng. Chem. Res.* **1997**, *36*, 4628−4637.
(32) Cui, G.; Li, Y.; Liu, J.; Wang, H.; Li, Z.; Wang, J. Tuning Environmentally Friendly Chelate-Based Ionic Liquids for Highly Efficient and Reversible SO2 Chemisorption. *ACS Sustainable Chem. Eng.* **2018**, *6*, 15292−15300.
(33) García, G.; Atilhan, M.; Aparicio, S. Assessment of DFT methods for studying acid gas capture by ionic liquids. *Phys. Chem. Chem. Phys.* **2015**, *17*, 26875−26891.
(34) Li, H.; Chang, Y.; Zhu, W.; Wang, C.; Wang, C.; Yin, S.; Zhang, M.; Li, H. Theoretical evidence of charge transfer interaction between SO2and deep eutectic solvents formed by choline chloride and glycerol. *Phys. Chem. Chem. Phys.* **2015**, *17*, 28729−28742.
(35) Sonnenberg, J. H.; Ehara, M.; Toyota, K.; Fukuda, R.; Hasegawa, J.; Ishida, M.; Nakajima, T.; Honda, Y.; Kitao, O. *Gaussian 09*, Revision C. 01; Gaussian, Inc.; Wallingford, CT, 2009.
(36) Lu, T.; Chen, F. Multiwfn: a multifunctional wavefunction analyzer. *J. Comput. Chem.* **2012**, *33*, 580−592.
(37) Cui, G.; Zhao, N.; Li, Y.; Wang, H.; Zhao, Y.; Li, Z.; Wang, J. Limited Number of Active Sites Strategy for Improving SO2 Capture by Ionic Liquids with Fluorinated Acetylacetonate Anion. *ACS Sustainable Chem. Eng.* **2017**, *5*, 7985−7992.

https://doi.org/10.1021/acs.jced.2c00334
J. Chem. Eng. Data 2022, 67, 3435−3442